

DOCUMENT CONTROL SHEET

	ORIGINATOR'S REF. NLR-TP-2003-124		SECURITY CLASS. Unclassified
ORIGINATOR National Aerospace Laboratory NLR, Amsterdam, The Netherlands			
TITLE Wake modelling accuracy requirements for prediction of rotor wake-stator interaction noise AIAA Paper 2003-3138			
PRESENTED AS: AIAA Paper 2003-3138 at the 9th AIAA/CEAS Aeroacoustics Conference, Hilton Head, South Carolina, USA, 12-14 May 2003			
AUTHORS P. Sijtsma and J.B.H.M. Schulten	DATE March 2003	PP 12	REF 14
ABSTRACT Rotor wake-stator interaction is an important element of aircraft engine noise, especially in the rear arc. For numerical predictions of this type of engine noise, an accurate rotor wake description is indispensable. However, for most CFD codes accurate calculation of the development of turbulent rotor wakes is not something natural. To assess the importance of wake modelling accuracy, the NLR lifting surface model was used for a parametric study. Many rotor wake-stator interaction calculations were made on a configuration with realistic dimensions. Systematic variations of wake depth, wake width, and axial and circumferential position of the wake origin were carried out. It was found that for 1 dB precision in the final acoustic result these parameters must have a relative accuracy varying from 6% to 12%. This is a real trial of strength for most CFD models. With the same 1 dB precision requirement, it was found that relative errors in the prediction of rotor viscous drag, which is an important factor in the wake development, are acceptable up to 23%.			



NLR-TP-2003-124


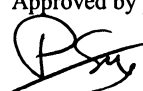

**Wake modelling accuracy requirements for
prediction of rotor wake-stator interaction noise**
AIAA Paper 2003-3138

P. Sijtsma and J.B.H.M. Schulten

This report is presented as AIAA Paper 2003-3138 at the 9th AIAA/CEAS
Aeroacoustics Conference, Hilton Head, South Carolina, USA, 12-14 May 2003.

The contents of this report may be cited on condition that full credit is given to NLR
and the authors.

Customer: National Aerospace Laboratory NLR
Working Plan number: A.1.C.3
Owner: National Aerospace Laboratory NLR
Division: Fluid Dynamics
Distribution: Limited
Classification title: Unclassified
March 2003

Approved by author:  27/03/03	Approved by project manager:  27/03/03	Approved by project managing department:  27/3/03
---	--	--



Contents

Nomenclature	3
I. Introduction	3
II. Lifting surface model	4
III. Geometry and flow conditions	5
Geometry	5
Flow conditions	5
Acoustic duct modes	5
IV. Datum model for viscous wakes	5
Wake model	5
Boundary condition	6
V. Wake variations	6
Basic variations	6
Variations in rotor drag	7
VI. Numerical results	7
Sound Power Levels	7
Datum wake	7
Basic variations	7
Variations in rotor drag	8
VII. Conclusions	8
Acknowledgement	8
References	9

21 Figures

(12 pages in total)

WAKE MODELLING ACCURACY REQUIREMENTS FOR PREDICTION OF ROTOR WAKE-STATOR INTERACTION NOISE

Pieter Sijtsma* and Johan B.H.M. Schulten†
National Aerospace Laboratory NLR, 8300 AD Emmeloord, The Netherlands

Rotor wake-stator interaction is an important element of aircraft engine noise, especially in the rear arc. For numerical predictions of this type of engine noise, an accurate rotor wake description is indispensable. However, for most CFD codes accurate calculation of the development of turbulent rotor wakes is not something natural. To assess the importance of wake modelling accuracy, the NLR lifting surface model was used for a parametric study. Many rotor wake-stator interaction calculations were made on a configuration with realistic dimensions. Systematic variations of wake depth, wake width, and axial and circumferential position of the wake origin were carried out. It was found that for 1 dB precision in the final acoustic result these parameters must have a relative accuracy varying from 6% to 12%. This is a real trial of strength for most CFD models. With the same 1 dB precision requirement, it was found that relative errors in the prediction of rotor viscous drag, which is an important factor in the wake development, are acceptable up to 23%.

Nomenclature

B	= number of rotor blades
c_d	= rotor blade section drag coefficient
\tilde{c}_d	= variation of c_d , Eq. (26)
c_R	= rotor chord length
h	= hub/tip ratio
k_{\max}	= maximum number of radial harmonics in Chebyshev polynomial expansions
S	= function describing blade surface, Eq. (12)
T_k	= Chebyshev polynomials, Eqs. (23), (24)
U	= axial flow speed
\vec{U}	= main flow
\vec{u}	= velocity distortion
\vec{u}_{induced}	= velocity distortion induced by stator response
\vec{u}_{wake}	= wake deficit velocity, Eq. (4)
V	= number of stator vanes
$x_{\text{le,S}}$	= axial position of stator leading edge
$x_{\text{te,S}}$	= axial position of stator trailing edge
$x_{\text{le,R}}$	= axial position of rotor leading edge
$x_{\text{te,R}}$	= axial position of rotor trailing edge
$\tilde{x}_{\text{te,R}}$	= variation of $x_{\text{te,R}}$, Eq. (20)

α	= angle defined by Eq. (7)
γ	= ratio of specific heats
χ_j	= Chebyshev polynomial expansion, Eq. (22)
γ_k^j	= coefficients in Chebyshev polynomial expansion, Eq. (22)
η	= traverse relative co-ordinate in rotor wake description, Eq. (6)
$\tilde{\eta}$	= variation of η , Eq. (19)
λ	= empirical constant in Eq. (4), $\lambda = 0.0222$
$\theta_{\text{te,R}}$	= circumferential position at $t = 0$ of rotor trailing edge
$\tilde{\theta}_{\text{te,R}}$	= variation of $\theta_{\text{te,R}}$, Eq. (21)
ρ	= density fluctuation
Ω	= rotor angular speed
ξ	= streamwise relative co-ordinate in rotor wake description, Eq. (6)
$\tilde{\xi}$	= variation of ξ , Eq. (18)

I. Introduction

An important element of turbomachinery noise is the interaction of rotor viscous wakes with a downstream stator vane row. The rotor wakes impinge on the stator vanes and induce an unsteady vane loading. This stator response is the physical source for the rotor-stator interaction noise. Acoustic duct modes, having a circumferential periodicity according to Tyler and Sofrin¹, are generated at multiples of the blade passing frequency. Both upstream and downstream radiating modes are generated. The

*Research Engineer, Aeroacoustics Department, P.O. Box 153, e-mail: sijtsma@nlr.nl.

†Research Fellow, retired 2002, e-mail: johan.schulten@planet.nl.



upstream modes are partly transmitted through and partly reflected by the rotor.

Since the pioneering study of Tyler and Sofrin¹ in the early 60's, a number of semi-analytic prediction models has been developed for rotor-stator interaction noise. Some of these are based on 2D approximations^{2,3}, others on a 3D lifting surface theory^{4,5}. The 2D methods have the drawback of ignoring spanwise interference; the 3D methods have the drawback of having to assume a uniform axial main flow. Thus, the 3D lifting surface models do not include the effects of swirl and vane stagger. The stator vanes have to be thin and aligned with the main, axial flow in the 3D methods and with the local flow in the 2D methods.

An alternative way to obtain rotor-stator interaction noise predictions is the application of CFD methods. Herewith, the aforementioned limitations of semi-analytic models can be overcome. Although CFD methods have their own drawbacks (long computing times and numerical artefacts), an important advantage of viscous CFD methods is their ability, at least in principle, to include the rotor wakes in the computation. Semi-analytic methods do not include viscosity and have to consider wakes as incident distortions. Normally, these wakes are computed from 2D idealised far wake models⁶ or, at best, taken from wake velocity measurements, which have their own inaccuracies. This paper is devoted to the question: how accurate must rotor wakes be computed in order to get reliable noise predictions? It was already shown by Schulten⁷ that stator response can be quite sensitive to rotor wake details.

For the assessment of these accuracy requirements, many rotor wake-stator interaction calculations have to be made with systematic variations in the rotor wake description. For that purpose, it is convenient to use a well-proven semi-analytic method, because modifications in the wake description can be introduced easily and the computing time is much less than for CFD methods. This paper describes a wake accuracy investigation carried out with the NLR method based on lifting surface theory⁴. This method was validated by several wind tunnel experiments in the period 1987 through 1995. A good agreement was found between theory and measurements^{8,9}. Furthermore, the method was compared to another lifting surface method⁵ in the 3rd CAA Workshop¹⁰. Again, good agreement was found between both methods, thereby establishing a firm benchmark case for CAA/CFD developers. Several numerical methods were tested on this benchmark, with very good results^{11,12,13}.

The results of this paper are based on a parametric study of many rotor wake-stator interaction calculations of a configuration with realistic dimensions. Typical 'Approach' flow and operating conditions were chosen. Variations in rotor wakes were made relative to a datum case, in which the wakes had a quasi-2D analytic description, based on Schlichting's turbulent wake model⁶. Systematic variations of wake depth, wake width, and axial and circumferential position of the wake origin were carried out.

In this paper, brief descriptions are given of the lifting surface model, the used geometry and the flow conditions. Then, the "datum" wake model is described, as well as the variations on that model. The numerical results are discussed and, finally, the conclusions are formulated.

II. Lifting surface model

The NLR model for predicting rotor-stator interaction noise is based on a lifting surface theory developed by Schulten⁴. In this theory, the flow is inviscid and isentropic. A uniform subsonic main flow is assumed, on which small distortions are superimposed. This main flow is supposed to be axial, so swirl is not included in this theoretical model. The blades of rotor and stator are modelled by lifting surfaces, i.e., by infinitely thin reference surfaces, across which steady and unsteady pressure discontinuities are allowed.

Most difficult part of the theory is to obtain the pressure jump across the reference surface, given an incident field. The pressure jump, or loading, Δp satisfies a Fredholm integral equation of the first kind, symbolically written:

$$\int K(z, \zeta) \Delta p(\zeta) d\zeta = f(z). \quad (1)$$

When unsteady loading is considered, the right hand side f follows from the incident field. For the steady loading problem, f also depends on angle of incidence, blade camber and blade thickness. The kernel K only depends on the fan operating conditions.

The unknown loading Δp is solved from Eq. (1), by expressing it as a series of suitably chosen basis functions and by applying a Galerkin projection. Then the unknown pressure coefficients can be solved from a linear system of equations:



$$\mathbf{LP} = \mathbf{R}, \quad (2)$$

where \mathbf{L} is a matrix of influence coefficients, \mathbf{P} is a vector of pressure coefficients and \mathbf{R} is a vector, which follows from the incident field.

III. Geometry and flow conditions

Geometry

In order to comply with the assumptions made in the lifting surface theory, the calculations are made for an annular duct geometry of constant cross-section. The rotor blades and the stator vanes have no thickness and do not disturb the axial main flow. Hence, the stator vanes are not staggered and the rotor blades follow helical surfaces defined by the ratio between rotor rotational speed and flow speed.

In the calculations for the present study, the axial positions of leading and trailing edges of rotor blades and stator vanes are independent of the radial position*. Thus, the axial chords of rotor and stator are constant along the span and, consequently, the true rotor chord increases from hub to tip.

The dimensions, which are based on a typical rotor-stator configuration, are:

$$\begin{aligned} \text{Number of rotor blades: } & B = 26, \\ \text{Number of stator vanes: } & V = 65, \\ \text{Hub/tip ratio: } & h = 0.569, \\ \text{Rotor leading edge: } & x_{le,R} = 0, \\ \text{Rotor trailing edge: } & x_{te,R} = 0.174, \\ \text{Stator leading edge: } & x_{le,S} = 0.433, \\ \text{Stator trailing edge: } & x_{te,S} = 0.546. \end{aligned}$$

The leading and trailing edge positions have been made dimensionless with the duct radius.

Flow conditions

For the axial flow speed U and the rotor angular speed Ω , typical 'Approach' conditions are used, with the following dimensionless values:

$$\begin{aligned} \text{Axial flow Mach number: } & U = 0.25, \\ \text{Rotor tip-Mach number: } & \Omega = 0.739. \end{aligned}$$

Acoustic duct modes

Under these conditions, the BPF is cut-off¹. Rotor-stator interaction modes are generated at frequencies $n \times \text{BPF}$, $n \geq 2$. In this study, we consider $2 \times \text{BPF}$ and $3 \times \text{BPF}$. Circumferential mode numbers m follow from the well-known Tyler and Sofrin rule:

$$m = nB - kV, \quad (3)$$

where n is the BPF harmonic number and k is an integer. Since $B = 26$ and $V = 65$, the most important modes are $m = -13$ at $2 \times \text{BPF}$ and $m = +13$ at $3 \times \text{BPF}$.

IV. Datum model for viscous wakes

Wake model

A quasi-2D Gaussian wake model⁶ is used. Just like the main flow, the wake model used here is not subject to swirl. Using a cylindrical co-ordinate system (x, r, θ) in which the x -direction is the direction of the main flow, the wake distortion velocity \vec{u}_{wake} is described by the following expression:

$$\vec{u}_{\text{wake}} = \begin{pmatrix} (u_{\text{wake}})_x \\ (u_{\text{wake}})_r \\ (u_{\text{wake}})_\theta \end{pmatrix} = \frac{1}{4} \sqrt{\frac{c_d c_R}{\pi \lambda \xi}} \exp\left(\frac{-\eta^2}{4 \lambda c_d c_R \xi}\right) \cdot \begin{pmatrix} -U \\ 0 \\ r\Omega \end{pmatrix}, \quad (4)$$

where

$$\begin{aligned} \lambda &= 0.0222 \text{ (empirical constant),} \\ c_d &= \text{section drag coefficient of rotor blade section,} \\ c_R &= \text{rotor chord length.} \end{aligned}$$

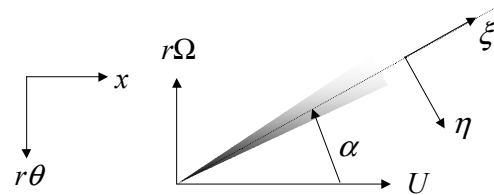


Fig. 1 Sketch of co-ordinate transformation

The streamwise relative co-ordinate ξ and the traverse relative co-ordinate η are defined by (see also Fig. 1)

$$\xi = (x - x_{te,R}) \cos(\alpha) - r(\theta - \theta_{te,R} - \Omega t) \sin(\alpha), \quad (5)$$

* This is not a limitation of the lifting surface theory.



$$\eta = (x - x_{te,R}) \sin(\alpha) + r(\theta - \theta_{te,R} - \Omega t) \cos(\alpha), \quad (6) \quad S(x, r, \theta, t) = 0. \quad (12)$$

where $\theta_{te,R}$ is the circumferential position at $t = 0$ of the trailing edge of a reference rotor blade. The angle α is given by

$$\alpha = \arctan(r\Omega/U). \quad (7)$$

Eq. (4) describes a velocity distortion that is Gaussian in the traverse co-ordinate η . The width of this Gaussian shape (the wake width) is determined by $\sqrt{c_d c_R \xi}$. Hence, the wake width increases with increasing streamwise co-ordinate ξ . In other words, the wake broadens as it moves downstream. Due to the square root factor in Eq. (4), which is proportional to the maximum velocity distortion (the wake depth), the total surface underneath the Gaussian curve does not vary with ξ , in accordance with the law of mass conservation.

The section drag coefficients c_d are calculated using Schlichting's formula for flat plate turbulent boundary layers⁶:

$$c_d = \frac{0.455}{\left[10 \log(\text{Re})\right]^{2.58}}, \quad (8)$$

in which Re is the Reynolds number:

$$\text{Re} = \frac{c_R U}{\nu_0}, \quad (9)$$

where ν_0 is the kinematic viscosity. The rotor chords can be calculated by:

$$c_R = (x_{te,R} - x_{le,R}) \sqrt{1 + (r\Omega/U)^2}. \quad (10)$$

Boundary condition

In the lifting surface theory, the following boundary condition has to be solved:

$$\left(\frac{\partial}{\partial t} + (\vec{U} + \vec{u}) \cdot \nabla\right) S = 0, \quad (11)$$

where \vec{U} is the main flow, \vec{u} is the distortion and S describes the blade surface by

In our flat plate case, where the stator vane surface is described by

$$S(x, r, \theta, t) = \theta - \text{Constant}, \quad (13)$$

Eq. (11) simplifies to

$$\vec{u} \cdot \nabla S = 0. \quad (14)$$

The velocity distortion \vec{u} can be written as the summation of the incident distortion \vec{u}_{wake} due to the viscous wakes, and the velocity \vec{u}_{induced} induced by the blade row response. Therefore, the equation to be solved is:

$$\vec{u}_{\text{induced}} \cdot \nabla S = -\vec{u}_{\text{wake}} \cdot \nabla S. \quad (15)$$

Using Eqs. (4) and (13), we have in Eq. (15):

$$\vec{u}_{\text{wake}} \cdot \nabla S = \frac{\Omega}{4} \sqrt{\frac{c_d c_R}{\pi \lambda \xi}} \exp\left(\frac{-\eta^2}{4 \lambda c_d c_R \xi}\right), \quad (16)$$

which defines the datum boundary condition for the present study.

V. Wake variations

Basic variations

In this section, it is described how variations in wake depth, wake width and wake origin are made on the datum wake boundary condition, Eq. (16).

We introduce radial functions $\chi_j(r)$, $j = 1, \dots, 4$, representing variations of the following:

χ_1 : relative wake depth,

χ_2 : relative wake width,

χ_3 : axial position of wake origin (= rotor trailing edge), relative to the rotor-stator gap,

χ_4 : circumferential position of wake origin, relative to the rotor blade spacing.

Instead of Eq. (16), we will now use:



$$\bar{u}_w \cdot \nabla S = (1 + \chi_1) \frac{\Omega}{4} \sqrt{\frac{c_d c_R}{\pi \lambda \xi}} \exp \left\{ - \left(\frac{\tilde{\eta}}{1 + \chi_2} \right)^2 / 4 \lambda c_d c_R \xi \right\}, \quad (17)$$

in which:

$$\xi = (x - \tilde{x}_{te,R}) \cos(\alpha) - r(\theta - \tilde{\theta}_{te,R} - \Omega t) \sin(\alpha), \quad (18)$$

$$\tilde{\eta} = (x - \tilde{x}_{te,R}) \sin(\alpha) + r(\theta - \tilde{\theta}_{te,R} - \Omega t) \cos(\alpha), \quad (19)$$

and

$$\tilde{x}_{te,R} = x_{te,R} + (x_{te,S} - x_{te,R}) \chi_3, \quad (20)$$

$$\tilde{\theta}_{te,R} = \theta_{te,R} + \frac{2\pi}{B} \chi_4 - \frac{\Omega}{U} (\tilde{x}_{te,R} - x_{te,R}). \quad (21)$$

The variation in axial position of the wake origin is such that the wake remains on the same helical surface. This is realised through the last term in the right hand side of Eq. (21).

The radial variations $\chi_j(r)$ are given as Chebyshev polynomial expansions:

$$\chi_j(r) = \sum_{k=0}^{k_{\max}} \gamma_k^j T_k \left(-1 + 2 \frac{r-h}{1-h} \right). \quad (22)$$

Chebyshev polynomials T_k (of the first kind) are defined by

$$T_k(\zeta) = \cos(k \arccos(\zeta)), \quad -1 \leq \zeta \leq 1, \quad (23)$$

or, equivalently, by

$$\begin{cases} T_0(\zeta) = 1, \\ T_1(\zeta) = \zeta, \\ T_k(\zeta) = 2\zeta T_{k-1}(\zeta) - T_{k-2}(\zeta), \quad k > 1. \end{cases} \quad (24)$$

Chebyshev polynomial functions are convenient for this purpose, because:

- They form a complete, orthogonal set (when using a modified L_2 -norm).
- The maximum (minimum) value of each polynomial T_k is 1 (-1), hence the coefficients γ_k^j correspond to the maximum absolute value of the polynomials $\gamma_k^j T_k$.

- The zero-order function T_0 represents constant distortion, the first order function T_1 represents linear distortion.

In this study, the coefficients γ_k^j are varied from $-1/2$ to $+1/2$. The highest radial harmonic considered in the present investigation is $k_{\max} = 2$.

Variations in rotor drag

Apart from the above-described basic wake variations, it is also interesting to consider variations in rotor section drag coefficient c_d , in other words, to consider

$$\bar{u}_{\text{wake}} \cdot \nabla S = \frac{\Omega}{4} \sqrt{\frac{\tilde{c}_d c_R}{\pi \lambda \xi}} \exp \left(\frac{-\eta^2}{4 \lambda \tilde{c}_d c_R \xi} \right), \quad (25)$$

in which

$$\tilde{c}_d = (1 + \chi_5) c_d \quad (26)$$

and, as in Eq. (22),

$$\chi_5(r) = \sum_{k=0}^{k_{\max}} \gamma_k^5 T_k \left(-1 + 2 \frac{r-h}{1-h} \right). \quad (27)$$

In fact, this wake variation can also be covered by the basic variations, by setting

$$(1 + \chi_1)^2 = (1 + \chi_2)^2 = 1 + \chi_5, \quad (28)$$

i.e., by controlled simultaneous variation of wake depth and wake width. Nevertheless, it is interesting to look at the drag coefficients separately, because errors in drag predictions may be due to inadequate modelling of the rotor boundary layer, instead of lack of accuracy in the calculation of the wake propagation.

VI. Numerical results

Sound Power Levels

The numerical results in this chapter are given as Sound Power Levels (PWL), defined by

$$\text{PWL} = 10^{10} \log(P) + 120 \text{ [dB]}, \quad (29)$$

where P is the acoustic power, which is the axial component of the acoustic intensity, integrated over a



duct cross-section. The acoustic intensity¹⁴ is the time-average of the acoustic energy flux \bar{I} , in dimensionless form:

$$\bar{I} = (\rho + \bar{U} \cdot \bar{u})(\bar{u} + \rho \bar{U}), \quad (30)$$

in which \bar{u} is the acoustic velocity (here: $\bar{u} = \bar{u}_{\text{induced}}$) and ρ is the corresponding acoustic density fluctuation. Summarised:

$$P = \iint_{h \leq r \leq 1} \langle I_x \rangle dS = \iint_{h \leq r \leq 1} \langle (\rho + U u_x)(u_x + \rho U) \rangle dS. \quad (31)$$

Datum wake

For the datum wake description, (16), the following PWL values (in dB and for full dimensions) were found:

	<u>2×BPF</u>	<u>3×BPF</u>
Downstream	120.0	111.3
Upstream	114.1	105.2

The results shown hereafter are relative to these datum values.

Basic variations

Results for the variation in relative wake depth (2×BPF & 3×BPF, upstream & downstream) are shown in Fig. 2 to Fig. 5. These figures show that a relative variation of 0.12 is allowed for errors in PWL less than 1 dB. In other words, the wake depth has to be calculated within 12% precision for a PWL accuracy of 1 dB. For other PWL precision demands, the wake depth accuracy requirements follow readily from the figures.

Results for the variation in relative wake width are shown in Fig. 6 to Fig. 9. The 2×BPF results (Fig. 6 and Fig. 8) are not very sensitive to variation, but the 3×BPF results (Fig. 7 and Fig. 9) show more variation. Roughly spoken, 6% precision in wake width modelling is required for 1 dB accurate PWL results.

Effects of variation in axial position of wake origin are plotted in Fig. 10 to Fig. 13. The lines with $k = 0$ represent straightforward variation of rotor-stator gap. The figures show that about 8% precision with respect

to rotor-stator gap is required for 1 dB accuracy in PWL.

Finally, results for variation in circumferential position of wake origin are shown in Fig. 14 to Fig. 17. Evidently, constant circumferential variation ($k = 0$) does not affect the Sound Power Levels. For higher radial harmonics of the variation, a precision of approximately 8% with respect to the rotor blade spacing is required for 1 dB accurate PWL results.

Variations in rotor drag

Results for variation in rotor section drag coefficient c_d are shown in Fig. 18 to Fig. 21. Variations in c_d imply simultaneous variations in wake depth and wake width (Eq. (28)). However, as follows from the figures, the accuracy requirements for c_d are much less restrictive than for wake depth and wake width individually. About 23% precision is required for 1 dB accuracy in PWL.

This is an interesting result, because errors in c_d may be due to wrong modelling of the rotor boundary layer, e.g. a wrong turbulence model, rather than lack of accuracy in the CFD calculation of the wake propagation. In other words, errors in c_d may persist, even though the propagation is calculated 100% accurately. Apparently, the penalty for errors made in the calculation of the wake propagation is higher than for errors in the rotor boundary layer model.

VII. Conclusions

A lifting surface model was used to assess the wake modelling accuracy requirements for accurate prediction of rotor wake-stator interaction noise. Rotor wake variations were made on a datum case of a realistic geometry under approach conditions. A quasi-2D analytic model for turbulent wake development was used to describe the datum wakes.

Variations in wake depth, wake width, and axial and circumferential position of the wake origin revealed the following accuracy requirements for PWL prediction within 1 dB precision:

- Wake depth: 12% (relative to depth of datum wake)
- Wake width: 6% (relative to width of datum wake)
- Axial origin: 8% (relative to rotor-stator gap)
- Circumferential origin: 8% (relative to rotor blade spacing)



For the rotor viscous drag, the relative accuracy required is 23%, which is less restrictive than the requirements above. Errors in viscous drag prediction may be due to the rotor boundary layer model instead of the wake propagation model. Apparently, it seems to be more important to have high numerical accuracy in the prediction of the wake development than in the description of the rotor boundary layer.

It is emphasised that the numbers presented here are based on variations on *one* case. This case is believed to be representative for CFD studies on similar configurations. Configurations that are different from the present case will probably show different numbers.

Acknowledgement

This study was carried out within the research project TurboNoiseCFD (Turbomachinery noise source CFD models for low noise aircraft designs), which was sponsored by the European Union. TurboNoiseCFD investigated the feasibility of the use of existing CFD or CAA methods for the numerical prediction of turbomachinery noise. One of the key objectives of the project was the formulation of the requirements of CFD codes for accurate turbomachinery noise predictions.

References

¹Tyler, J.M., and Sofrin, T.G., "Axial flow compressor noise studies", *SAE Transactions*, Vol. 70, pp. 309-332, 1962.
²Fleeter, S., "Fluctuating lift and moment coefficients for cascaded airfoils in a nonuniform compressible flow", *Journal of Aircraft*, Vol. 10, No. 2, pp. 93-98, 1973.
³Parry, A.B., "A modular prediction scheme for blade row interaction noise", AIAA Paper 95-024, 1995.
⁴Schulten, J.B.H.M., "Sound generation by ducted fans and propellers as a lifting surface problem", PhD thesis, University of Twente, 1993.
⁵Namba, M., "Lifting surface theory for a rotating subsonic or transonic blade row", *British Reports & Memoranda*, No. 3740, 1972.
⁶Schlichting, H., *Boundary layer theory*, McGraw-Hill, 1979.
⁷Schulten, J.B.H.M., "Unsteady leading-edge suction effects on rotor-stator interaction noise", *AIAA Journal*, Vol. 38, No. 9, pp. 1579-1585, 2000, also NLR TP 99064.
⁸Schulten, J.B.H.M., "Experimental validation of a lifting surface model for rotor wake-stator interaction", AIAA Paper 89-1125, 1989.

⁹Sijtsma, P., Rademaker, E.R., and Schulten, J.B.H.M., "Experimental validation of a lifting surface theory for rotor-stator interaction noise generation", *AIAA Journal*, Vol. 36, No. 6, pp. 900-906, 1998 also NLR TP 96122.
¹⁰Namba, M., and Schulten, J.B.H.M., "Numerical results of lifting surface theory", Cat. 4 benchmark problem, 3rd CAA Workshop, 2000.
¹¹Wilson, A.G., "Application of CFD to Wake/Aerofoil Interaction Noise – A Flat plate Validation Case", AIAA Paper 2001-2135, 2001.
¹²Elhadidi, B., and Atassi, H.M., "Sound Generation and Scattering from Radial Vanes in Uniform Flow", Paper AAC-03, 7th Int. Conf. of Fluid Dyn. and Propulsion, Sharm El-Sheikh, Egypt, 2001.
¹³Prasad, D., and Verdon, J.M., "A three-dimensional linearized Euler analysis of classical wake/stator interactions: validation and unsteady response predictions", *Int. Journal of Aeroacoustics*, Vol.1, No.2, pp. 137-163, 2002.
¹⁴Goldstein, M.E., *Aeroacoustics*, McGraw-Hill, 1976.

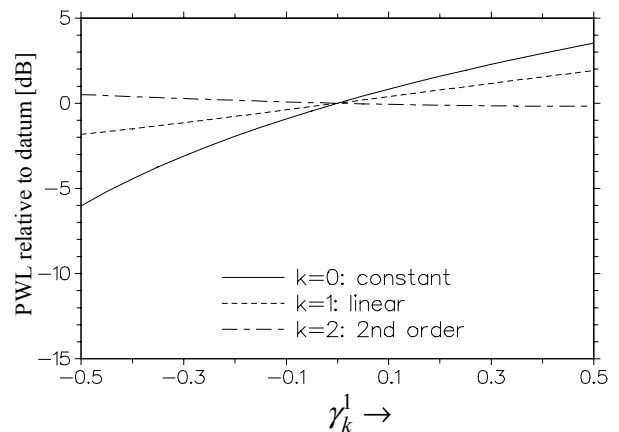


Fig. 2 Effects of variations in relative wake depth on downstream radiating sound power, 2×BPF, m = -13

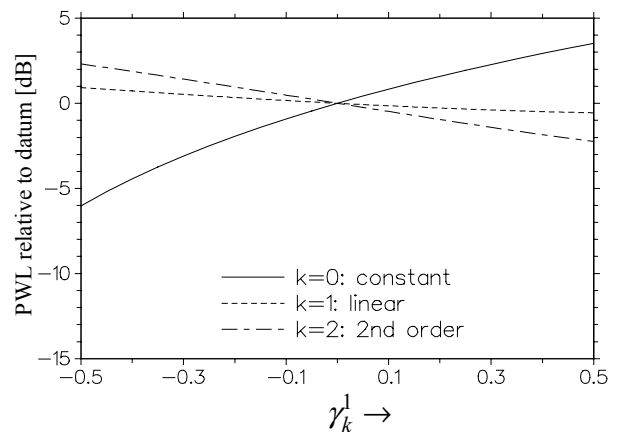


Fig. 3 Effects of variations in relative wake depth on downstream radiating sound power, 3×BPF, m = +13

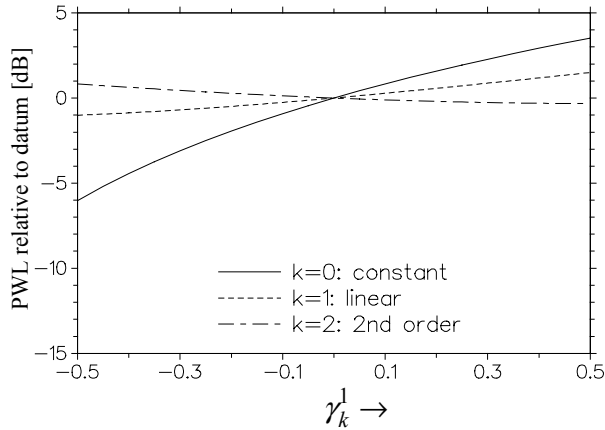


Fig. 4 Effects of variations in relative wake depth on upstream radiating sound power, 2xBPF, $m = -13$

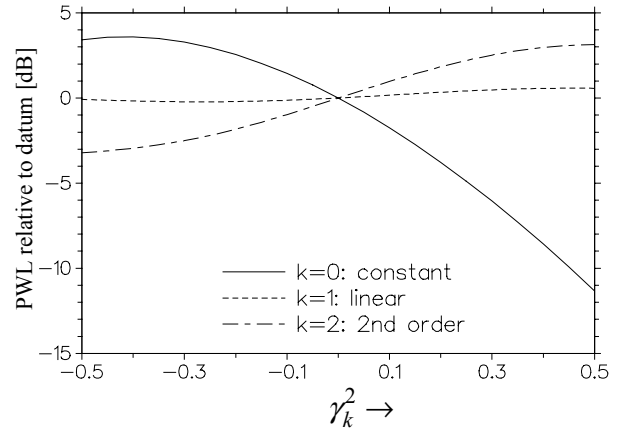


Fig. 7 Effects of variations in relative wake width on downstream radiating sound power, 3xBPF, $m = +13$

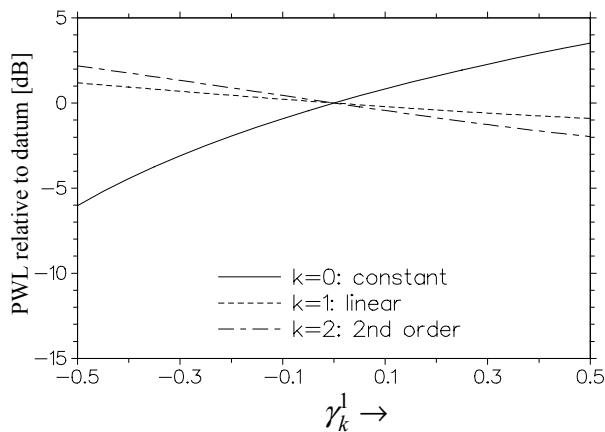


Fig. 5 Effects of variations in relative wake depth on upstream radiating sound power, 3xBPF, $m = +13$

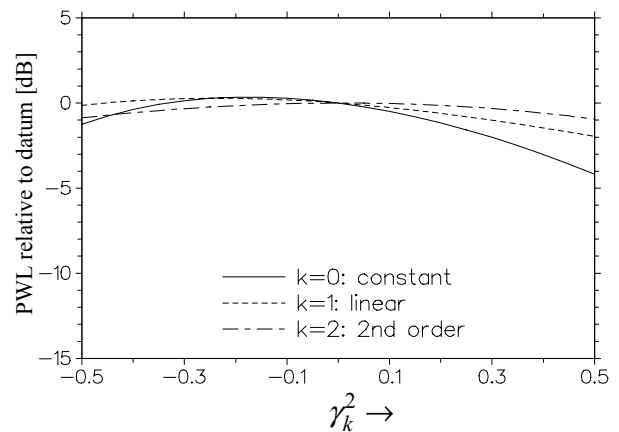


Fig. 8 Effects of variations in relative wake width on upstream radiating sound power, 2xBPF, $m = -13$

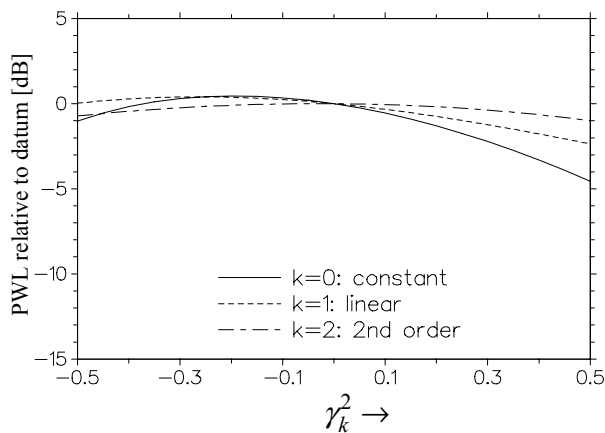


Fig. 6 Effects of variations in relative wake width on downstream radiating sound power, 2xBPF, $m = -13$

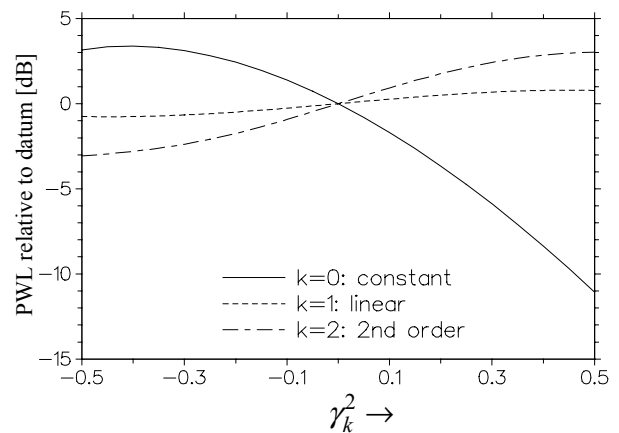


Fig. 9 Effects of variations in relative wake width on upstream radiating sound power, 3xBPF, $m = +13$

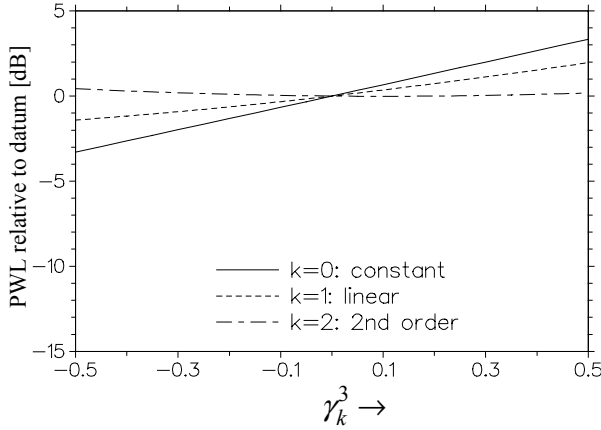


Fig. 10 Effects of variations in axial position of wake origin, relative to rotor-stator gap, on downstream radiating sound power, 2xBPF, $m = -13$

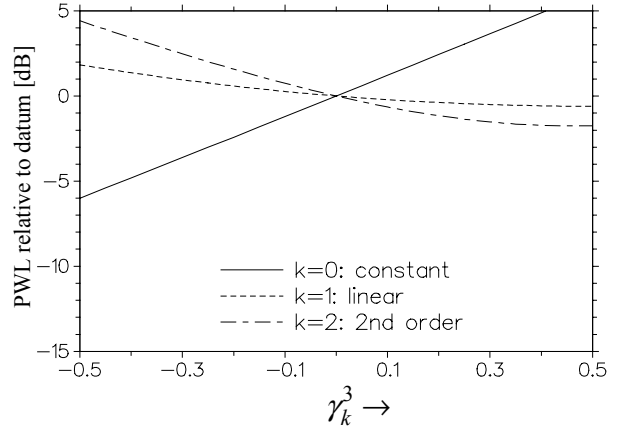


Fig. 13 Effects of variations in axial position of wake origin, relative to rotor-stator gap, on upstream radiating sound power, 3xBPF, $m = +13$

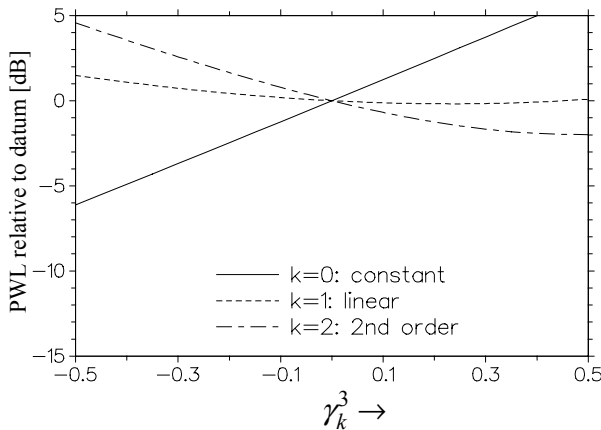


Fig. 11 Effects of variations in axial position of wake origin, relative to rotor-stator gap, on downstream radiating sound power, 3xBPF, $m = +13$

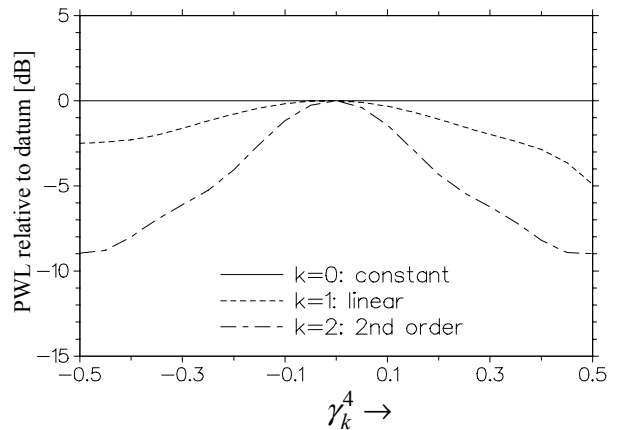


Fig. 14 Effects of variations in circumferential position of wake origin, relative to rotor blade spacing, on downstream radiating sound power, 2xBPF, $m = -13$

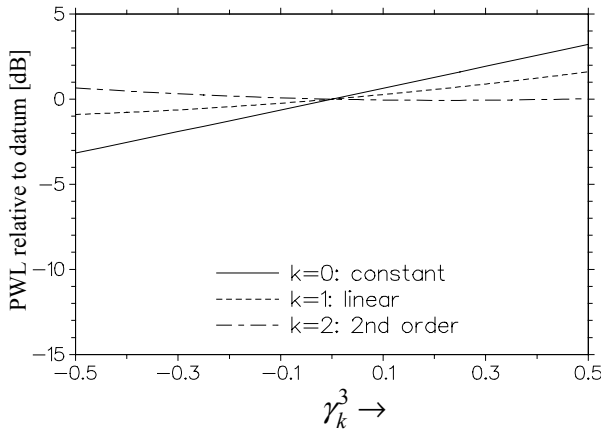


Fig. 12 Effects of variations in axial position of wake origin, relative to rotor-stator gap, on upstream radiating sound power, 2xBPF, $m = -13$

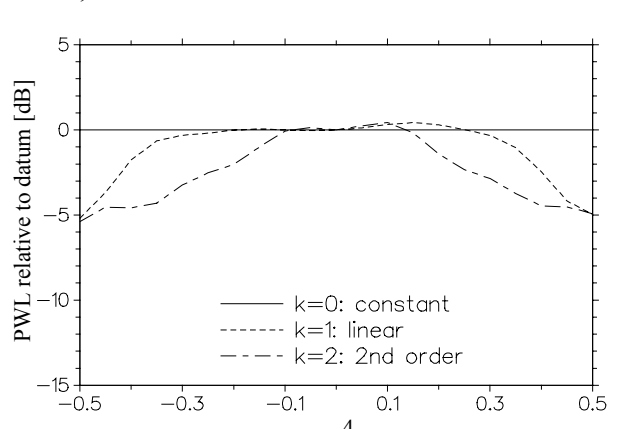


Fig. 15 Effects of variations in circumferential position of wake origin, relative to rotor blade spacing, on downstream radiating sound power, 3xBPF, $m = +13$

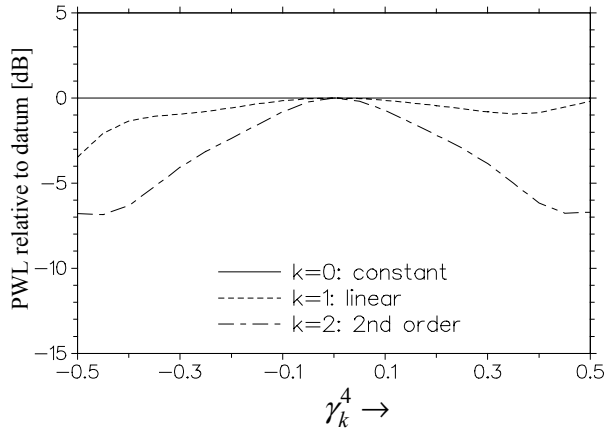


Fig. 16 Effects of variations in circumferential position of wake origin, relative to rotor blade spacing, on upstream radiating sound power, 2×BPF, $m = -13$

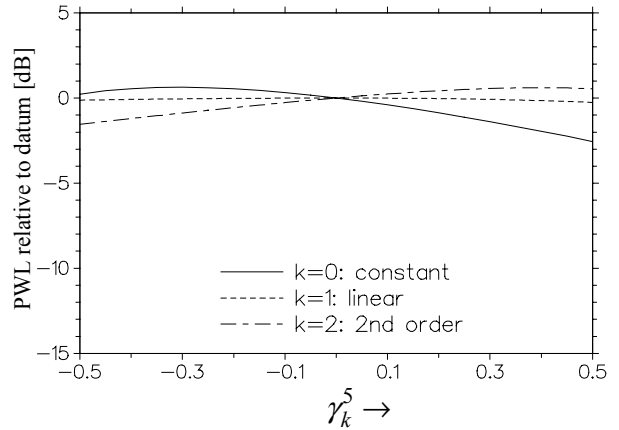


Fig. 19 Effects of variations in section drag coefficient on downstream radiating sound power, 3×BPF, $m = +13$

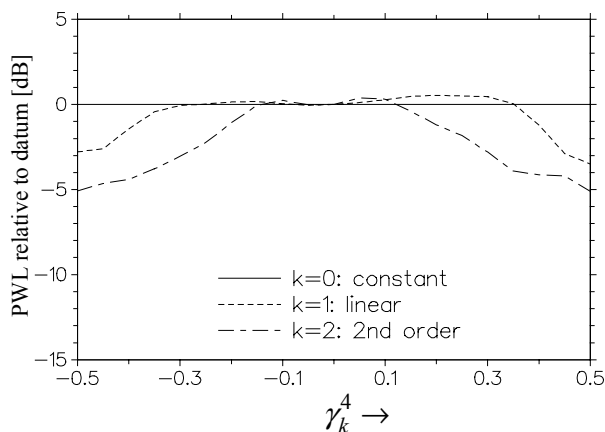


Fig. 17 Effects of variations in circumferential position of wake origin, relative to rotor blade spacing, on upstream radiating sound power, 3×BPF, $m = +13$

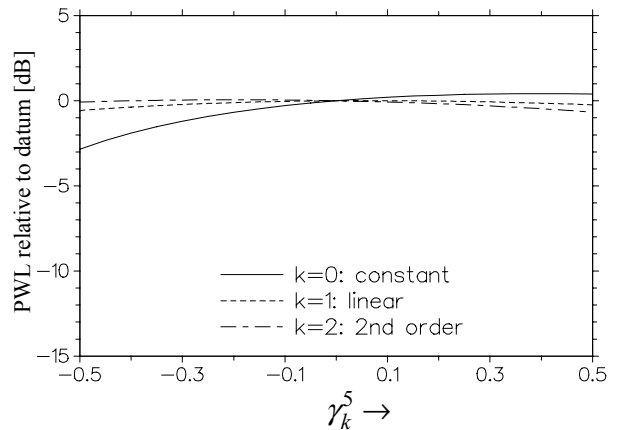


Fig. 20 Effects of variations in section drag coefficient on upstream radiating sound power, 2×BPF, $m = -13$

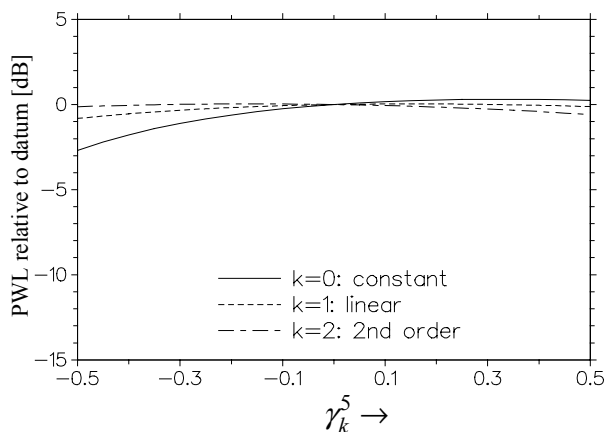


Fig. 18 Effects of variations in section drag coefficient on downstream radiating sound power, 2×BPF, $m = -13$

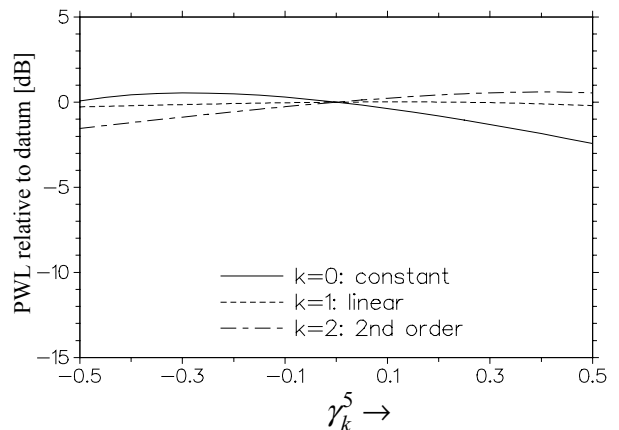


Fig. 21 Effects of variations in section drag coefficient on upstream radiating sound power, 3×BPF, $m = +13$